

Layer features of the lattice gas model for self-organized criticality

N. C. Pesheva,^{1,*} J. G. Brankov,¹ and E. Canessa²

¹*Institute of Mechanics, Bulgarian Academy of Sciences, Academician Georgy Bonchev Street 4, 1113 Sofia, Bulgaria*

²*International Centre for Theoretical Physics, Trieste, Italy*

(Received 13 July 1995)

A layer-by-layer description of the asymmetric lattice gas model for $1/f$ noise suggested by Jensen [Phys. Rev. Lett. **64**, 3103 (1990)] is presented. The power spectra of the lattice layers in the direction perpendicular to the particle flux is studied in order to understand how the white noise at the input boundary evolves, on the average, into $1/f$ noise for the system. The effects of high boundary drive and uniform driving force on the power spectrum of the total number of diffusing particles are considered. In the case of nearest-neighbor particle interactions, high statistics simulation results show that the power spectra of single lattice layers are characterized by different β_x exponents such that $\beta_x \rightarrow 1.9$ as one approaches the outer boundary.

PACS number(s): 05.40.+j, 74.40.+k, 64.60.Ht, 73.50.Td

Lattice gas models play an important role in exploring self-organized criticality (SOC) [1], which is an attempt to find a general unifying principle explaining the ubiquity of $1/f$ noise and fractality in nature. The idea behind these studies is that $1/f$ spectra occur when many-body dissipative systems evolve naturally (without a fine tuning of some parameter) toward a set of states without a characteristic length and/or time scale [2–6]. The basic feature of $f^{-\beta}$ noise, with $\beta \approx 1$, is the long range and self-similarity of the temporal fluctuations of some physical quantity such as the total number of diffusing particles $N(t)$.

In particular, the asymmetric lattice gas (ALG) model introduced by Jensen [2] allows us to describe $1/f$ noise in a highly interacting system of particles following diffusive dynamics. The ALG model can be considered as a transformer which produces a highly correlated signal out of a white noise (or completely uncorrelated signal) at the input boundary. It has a simple physical interpretation as a model of transport phenomena in type-II superconductors.

In an attempt to understand how the SOC phenomena arise in lattice gas models, such as the ALG model, it is also necessary to carry out a more detailed analysis in terms of the power spectra of the individual layers in the model. This is the main goal of this paper.

Here we present a layer-by-layer description of Jensen's ALG model for $1/f$ noise by studying the power spectra of the lattice layers in the direction perpendicular to the particle flux. We studied how the white noise at the input boundary evolves throughout the lattice, characterized by different exponents β_x , such that the critical exponent β for the total number of particles (and large times) is close to 1, as found by Jensen [2]. The effects of high boundary drive and uniform driving force

on the power spectrum of the total number of diffusing particles are also considered.

The lattice gas cellular automaton model of Jensen [2] is a system of particles residing on a square lattice Λ of $N_x \times N_y$ lattice sites. The particles obey an exclusion principle, so that there is no more than one particle on a given site at time t . With every site $\vec{r} \in \Lambda$ a variable $n(\vec{r}; t)$ taking values 0 and 1 is associated. As usual, $n(\vec{r}; t) = 1$ means that there is a particle on site \vec{r} at time t and $n(\vec{r}; t) = 0$ that the site is empty. The particles on nearest-neighbor sites repel each other with a central force of strength J , i.e.,

$$\vec{F}_{\text{int}}(n(\vec{r}; t)) = -Jn(\vec{r}; t) \sum_{i=1}^q n(\vec{r} + \vec{e}_i; t) \vec{e}_i, \quad (1)$$

where \vec{e}_i , $i = 1, \dots, q$ are the unit vectors to the nearest neighbors (in the calculations we set $J = 1$). In the more general case an additional driving force $\vec{F}_{\text{dr}}(\vec{r})$ could be applied to the particles, so that the total force acting on a particle is

$$\vec{F}_{\text{tot}}(\vec{r}) = \vec{F}_{\text{int}}(\vec{r}) + \vec{F}_{\text{dr}}(\vec{r}). \quad (2)$$

The system evolves at discrete time steps following diffusive deterministic dynamics. The configuration $\{n(\vec{r}; t)\}_{\vec{r} \in \Lambda}$ of the system is updated simultaneously. Every particle l is moved one lattice site in the direction of the resulting force, so that the coordinates of the particle are

$$\vec{r}_l(t+1) = \vec{r}_l(t) + \vec{d}_l(t), \quad (3)$$

where \vec{d} is the displacement vector, determined by

$$d_x = \left\lceil \frac{F_x}{F} \right\rceil, \quad d_y = \left\lceil \frac{F_y}{F} \right\rceil. \quad (4)$$

Here $F = |\vec{F}|$ and the square brackets $\lceil \]$ mean taking the nearest integer to the number enclosed in the brackets. Equation (3) in combination with (4) implies that diago-

*Electronic address: nina@bgearn.bitnet

nal moves are also allowed.

To ensure single occupancy of a lattice site, some additional rules, termed by Jensen [2] blocking mechanisms, are applied. These are the following.

(1) If the site to which a particle attempts to move is occupied, the particle is not moved.

(2) If there are two particles which attempt to move to the same lattice site, the particle to which a larger force is applied wins; if the forces are equal, neither particle moves.

The boundary conditions are asymmetric. It is assumed that at the left side of the system [i.e., at $(0, y)$] there is a layer of fixed particles. The role of this layer is to push the particles in the first column $(1, y)$ into the system. At every time step the particles in the first column are first removed, and then particles are introduced with a probability p , called the boundary drive. In this work, the effect of the lattice boundary drive p is studied over a large range of possible values $(0-1)$. The particles can freely leave the system over the right edge. Periodic boundary conditions are imposed in the y direction. This leads to a net flux of particles through the system.

The power spectrum $S_N(f)$ of the total number of particles in the system is defined in a standard way as [7,8]

$$S_N(f) = \lim_{T \rightarrow \infty} \frac{2}{T} \langle |X(f, T)|^2 \rangle, \quad (5)$$

where $X(f, T)$ is the finite Fourier transform of $N(t)$ [from sample sequences $N(t_i)$, $i=1, \dots, T$] given by

$$X(f, T) = \int_0^T N(t) e^{-i2\pi f t} dt, \quad (6)$$

and the angular brackets $\langle \rangle$ denote averaging over many realizations of the process.

If the process is stationary, $S_N(f)$ can be expressed in terms of the autocorrelation function of the time signal $R_N(\tau) = \lim_{T \rightarrow \infty} (1/T) \int_0^T \langle N(t)N(t+\tau) \rangle dt$ (the so-called Wiener-Khintchin theorem)

$$S_N(f) = 4 \int_0^\infty R_N(\tau) \cos(2\pi f \tau) d\tau. \quad (7)$$

We now focus on the results obtained for the system from the present simulations. Our simulations confirm that the power spectrum has a power law dependence on the frequency in a wide interval of frequencies, i.e., $S_N(f) \sim 1/f^\beta$, with β roughly equal to 1. As can be seen from Fig. 1, at small frequencies $f < f_c$, there is a cross-over to a white noise [$S_N(f) \sim \text{const.}$] due to the finite system size. Indeed, f_c decreases with increasing the system size as $\sim 1/N_x^2$ as predicted in [9] but with different proportionality constant.

Having in mind that when the system size $N_x \rightarrow \infty$ the power spectrum is expected to be $\sim 1/f^\beta$, we approximate the power spectrum for the finite system by

$$F(f) = \frac{A}{[1 + (f/f_c)^2]^{\beta/2}}, \quad (8)$$

where A , f_c , and β are fitting parameters. We find that the best fit to our results for several system sizes $N_x \times 8$ and $N_x = 10, 20, 30, 40, 50$, and 100 for A , f_c , and β gives

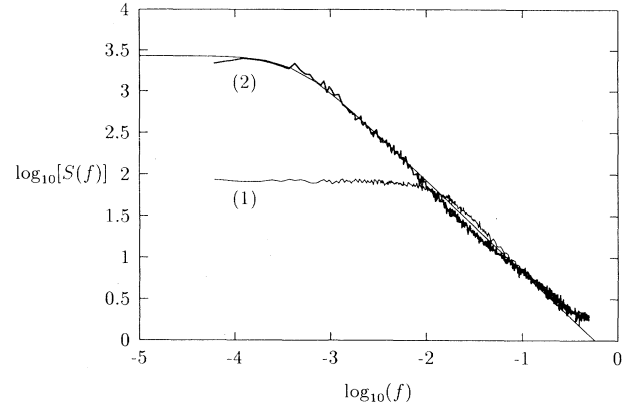


FIG. 1. Log-log plot of the power spectra $S_N(f)$ of the total number of particles against frequency f at low boundary drive $p=0.2$ and no driving force: curve (1) is for a system of size 10×8 , and curve (2) is for a system of size 50×8 together with the continuous fitting function $F(f)$.

$$A \approx 0.604 f_c^{-\beta}, \quad \beta \approx 1.09, \quad (9)$$

as one would expect from Eq. (8).

When we change the boundary drive p between 0 and 1, β is found to vary slightly. However, the limits $p \rightarrow 0$ and $p \rightarrow 1$ need special attention. For the case $p \rightarrow 0$, as studied in Refs. [2,9], a transition toward $\beta \approx 2$ was reported. For a high boundary drive, e.g., $p=0.99$, we found $\beta \approx 1.4$, as compared to $\beta \approx 1.05$ when $p=0.90$ for the same system size. Our simulation results also show that for a high boundary drive there exists a tendency of β to grow as the system size is increased. For $p=0.9$ and size 60×48 , we find $\beta \approx 1.4$ as compared to $\beta \approx 1.05$ for the small 10×8 system.

In the limiting case $p=1$ the system is completely deterministic, and can be studied analytically. The power spectrum is changed to a different type, consisting only of a few characteristic frequencies. For a system of length $N_x=8$, the spectrum consists of the set of frequencies $\{0, 0.125, 0.250, 0.375, 0.5\}$. The presence of even a very small stochastic element in the boundary drive, i.e., $p \rightarrow 1$, but $p \neq 1$, produces a qualitatively different picture.

Let us now continue studying the individual layers in the asymmetric lattice gas model under consideration. The averaged occupancy of a layer of the lattice $\langle \bar{n}(x) \rangle$ is defined as

$$\langle \bar{n}(x) \rangle = \left\langle \frac{1}{T} \sum_{i=1}^T \sum_{y=1}^{N_y} n(x, y, t_i) \right\rangle, \quad x=1, \dots, N_x. \quad (10)$$

At low boundary drive $p=0.2$, we obtain a typical saw-like shape of the density profile for small lattice sizes. At this value of p the average density of particles in the statistically stationary state of the system remains low, $\rho \approx 0.28$. Since the particles repel each other, states with alternating high occupancy layers and low occupancy layers are encountered more often. As the system size is increased the density distribution becomes more smooth, as shown in Fig. 2, but it cannot be well approximated by

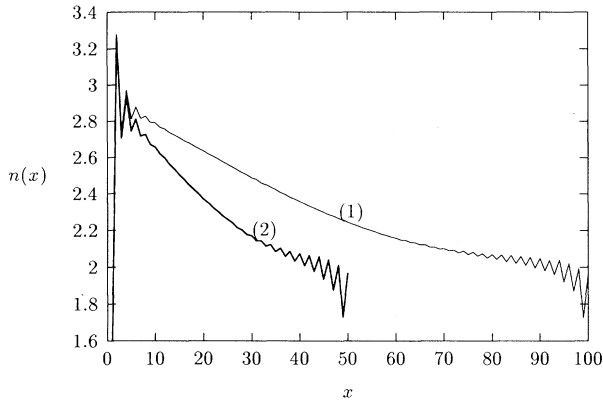


FIG. 2. The average occupancy of a column $\langle n(x) \rangle$ vs column number for a system 100×8 [curve (1)] and for a system 50×8 [curve (2)] at $p=0.2$.

the linear distribution with constant gradient, as discussed in [2]. An increase in the boundary drive smooths the density distribution. We add that the application of a driving force lowers the average occupancy in the system, as compared to the case without driving force.

At low boundary drive, the application of a small uniform driving force destroys the $1/f^\beta$ type of power spectrum, as seen in Fig. 3. For $F_{dr} > F_{cr}$, where $F_{cr} \approx 1.75$, the power spectrum is the same as for a noninteracting system (except for the hard-core exclusion) as shown in Fig. 4. At higher values of the boundary drive and small driving force, the power spectrum again displays $1/f^\beta$ behavior in a small frequency interval. Therein β takes a value ($\beta \approx 1.6$) larger than in the case without driving force ($\beta \approx 1.05$), as shown in Fig. 5. This behavior could possibly be explained in the following way. The higher boundary drive ($p=0.9$) produces a higher average density in the system. A higher density leads to stronger

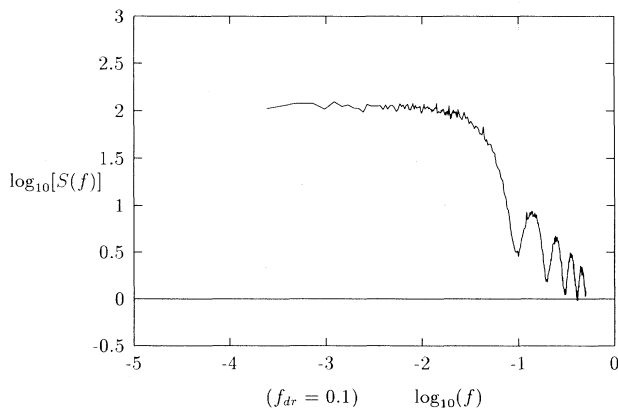


FIG. 3. The effect of a small uniform driving force $F_{dr}=0.1$ on the power spectrum for a system 10×8 at small boundary drive $p=0.2$.

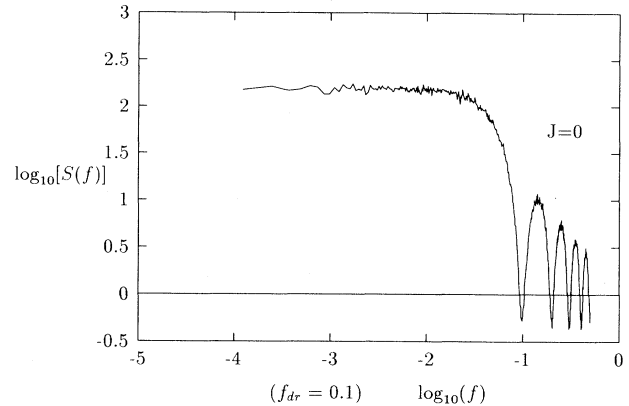


FIG. 4. The effect of a small uniform driving force $F_{dr}=0.1$ on the power spectrum for a system 10×8 of a noninteracting system (hard-core interaction only).

correlations, and damps the effect of the driving force. This point needs further elucidation in view of the analytical results obtained from the Langevin equation [10].

At a moderate boundary drive, $p=0.2$, the autocorrelation functions and the individual power spectra of the layers are studied for different lattice sizes, $N_x \times 8$, where $N_x = 10, 20, 30, 50$, and 100 , and also 60×48 . The power spectrum of the number of particles in a layer, $S_{L_x}(f)$, has a form similar to that for the total number of particles in the system, as seen in Fig. 6. The critical frequency f_c at which a crossover to white noise occurs depends on the layer selected, i.e., $f_c = f_c(x)$. The width of the frequency interval Δf , in which $1/f^\beta$ holds, also depends on the position x . As $x \rightarrow N_x$, the crossover frequency changes toward higher frequency values, and the interval $\Delta f(x)$ broadens. It is interesting to note that even the

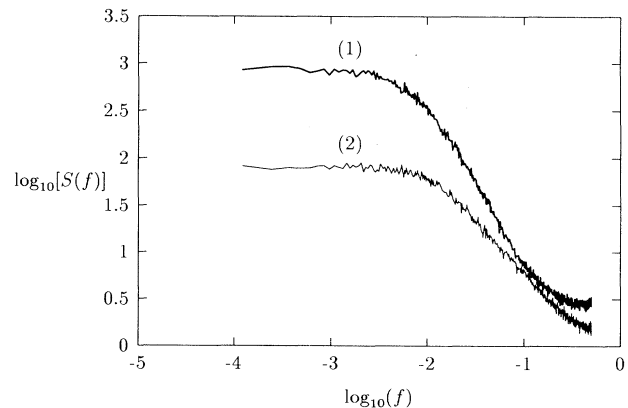


FIG. 5. Log-log plot of the power spectra of a system 10×8 at high boundary drive $p=0.9$: curve (1) for $F_{dr}=0.1$ ($\beta \approx 1.6$), and curve (2) for $F_{dr}=0$ ($\beta \approx 1.05$).

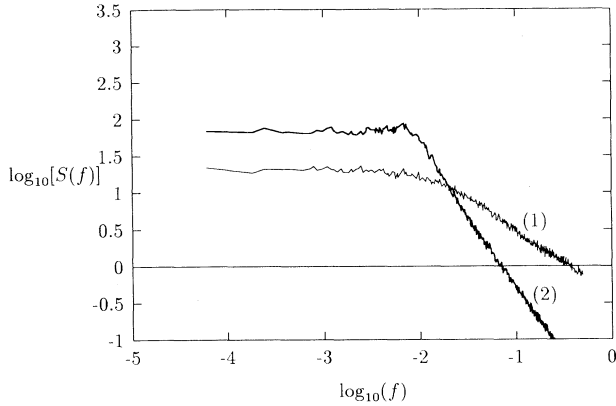


FIG. 6. Log-log plot of the power spectra of two layers of a system of size 30×8 are shown: curve (1) is the power spectrum of the middle layer— $x = 15$ ($\beta \sim 0.95$); and curve (2) of the last layer— $x = 30$ ($\beta \sim 1.9$).

first layer (immediately after the input boundary layer—whose power spectrum corresponds to white noise) already has $\beta \approx 0.8$, though in a very narrow frequency interval.

We have calculated the autocorrelation functions $R_{L_x}(\tau)$ of the system layers (shown in Fig. 7) by averaging $N_{L_x}(t)N_{L_x}(t+\tau)$ over one simulation, and then averaging over many (up to 1000) independent simulations for different system sizes. $R_{L_x}(\tau)$ of the single layers are found to decay much slower than the autocorrelation function of the whole system. As discussed in Ref. [11], finite system effects on $R_{L_x}(\tau)$ should be taken into account to obtain the proper behavior for the infinite system.

In Fig. 8, β_r data for several system sizes are shown as a function of the normalized layer distance within the lattice $r = x/N_x$. We find that the exponent of the last layer

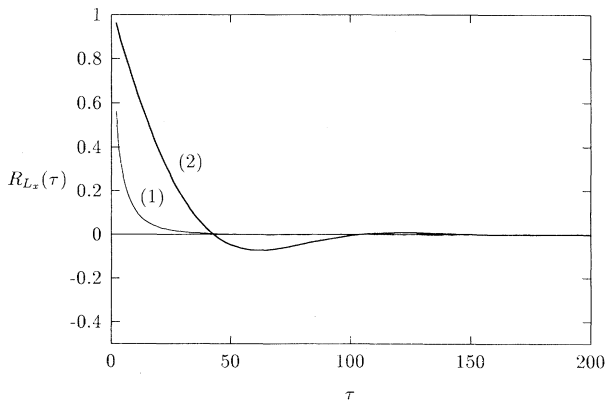


FIG. 7. The normalized autocorrelation functions $R_{L_x}(\tau)$ corresponding to the power spectra in Fig. 6: curve (1) is the autocorrelation function of the middle layer $x = 15$, and curve (2) is the autocorrelation function of the last layer $x = 30$.

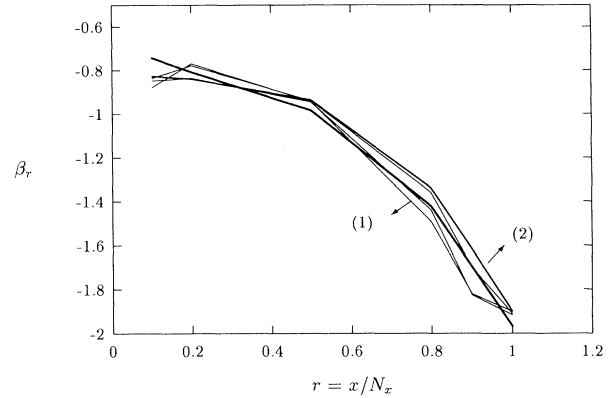


FIG. 8. The dependence of the critical exponent β_r on the relative distance of a layer number r at moderate boundary drive $p = 0.2$ for system sizes $N_x \times 8$ with $N_x = 20, 30, 40, 50$, and 100. Curve (1) is for a 20×8 system, and curve (2) is for a 100×8 system.

is $\beta(r=1) \approx 1.9$ —a result very close to the well known result for the Wiener process. Furthermore we also see that, within numerical accuracy (less than $\sim 5\%$ error), all β_r lie on approximately the same curve. Thus we find that while the individual power spectra of the layers are different and characterized with different β_x , their collective behavior produces a power spectrum for the total number of particles in the system with $\beta \approx 1.1$ (Fig. 1).

We also studied the effect of applying a nonuniform driving force on the power spectrum of the total number of particles in the ALG. For a moderate boundary drive ($p = 0.2$) we applied an additional driving force with a constant gradient $\Delta F_{\text{dr}} = 0.1$. We find that the effect on the power spectrum is much less pronounced than in the case of a uniform driving force. In fact one can still approximate the spectrum by $1/f^\beta$, but now $\beta \approx 1.2$ for a system of size 10×8 as compared to $\beta \approx 1.05$ for the same system without shear.

In conclusion we summarize our numerical findings. In an attempt to understand how SOC arises in simple lattice gas models of many particles systems, we have carried out a more detailed analysis of the ALG model in terms of the power spectra of the individual layers in a direction perpendicular to the particle flux. The effects of high boundary drive and uniform driving force on the power spectrum of the total number of diffusing particles have been also considered. In particular, our results for the limiting case $p \rightarrow 1$ supplement previous work [2]. Our findings reveal some interesting features for the spatial variation of the (local) exponents β_x . The layer after the boundary layer with the white noise power spectrum is found to display an exponent $\beta(x=2) \approx 0.8$ in a very narrow frequency interval, whereas we find that the exponent of the last layer is $\beta(r=1) \approx 1.9$.

N.C.P. gratefully acknowledges financial support from the ICTP, Trieste, where this work was started. This work was also supported by the Bulgarian National Foundation for Scientific Research Grant No. MM-405/94.

- [1] P. Bak, C. Tang, and K. Wiesenfeld, *Phys. Rev. Lett.* **59**, 381 (1987); *Phys. Rev. A* **38**, 364 (1988).
- [2] H. J. Jensen, *Phys. Rev. Lett.* **64**, 3103 (1990); *Mod. Phys. Lett. B* **5**, 625 (1991); *Phys. Scr.* **43**, 593 (1991).
- [3] R. Voss, *Phys. Rev. Lett.* **68**, 3805 (1992).
- [4] J. Stephany, *Phys. Rev. B* **46**, 12 175 (1992).
- [5] E. Canessa, *Phys. Rev. E* **47**, 5 (1993).
- [6] H. Rosu and E. Canessa, *Phys. Rev. E* **47**, R3818 (1993).
- [7] J. S. Bendat and A. G. Piersol, *Random Data: Analysis and Measurement Procedures* (Wiley, New York, 1971).
- [8] E. Bonabeau and P. Lederer, *J. Phys. A* **27**, L243 (1994).
- [9] T. Fiig and H. J. Jensen, *J. Stat. Phys.* **71**, 653 (1993).
- [10] G. Grinstein, T. Hwa, and H. J. Jensen, *Phys. Rev. A* **45**, R559 (1992).
- [11] O. I. Yordanov and N. I. Nickolaev, *Phys. Rev. E* **49**, R2517 (1994).